water

MDPI

Article

Improving Formaldehyde Removal from Water and Wastewater by Fenton, Photo-Fenton and Ozonation/Fenton Processes through Optimization and Modeling

Ahmad Hosseinzadeh [1], Ali Asghar Najafpoor [2], Ali Asghar Navaei [2,*], John L. Zhou [1,*], Ali Altaee [1], Navid Ramezanian [3], Aliakbar Dehghan [2], Teng Bao [1,4] and Mohsen Yazdani [5]

1 Centre for Green Technology, School of Civil and Environmental Engineering, University of Technology, Sydney, NSW 2007, Australia; seyedahmad.hosseinzadeh@student.uts.edu.au (A.H.); ali.altaee@uts.edu.au (A.A.); tengbao1222@sina.com (T.B.)
2 Social Determinants of Health Research Center, Department of Environmental Health Engineering, Mashhad University of Medical Sciences, Mashhad 9138813944, Iran; NajafPoorAA@mums.ac.ir (A.A.N.); aliakbardehghan@gmail.com (A.D.)
3 Department of Chemistry, Faculty of Science, Ferdowsi University of Mashhad, Mashhad 9177948974, Iran; ramezanian@um.ac.ir
4 School of Biology, Food and Environment Engineering, Hefei University, Hefei 230000, China
5 Student Research Committee, Department of Environmental Health Engineering, School of Public Health, Ahvaz Jundishapur University of Medical Sciences, Ahvaz 6135733184, Iran; hosseinzadeh26@gmail.com
* Correspondence: a.navaei2016@gmail.com (A.A.N.); junliang.zhou@uts.edu.au (J.L.Z.)

check for updates

Citation: Hosseinzadeh, A.; Najafpoor, A.A.; Navaei, A.A.; Zhou, J.L.; Altaee, A.; Ramezanian, N.; Dehghan, A.; Bao, T.; Yazdani, M. Improving Formaldehyde Removal from Water and Wastewater by Fenton, Photo-Fenton and Ozonation/Fenton Processes through Optimization and Modeling. *Water* **2021**, *13*, 2754. https://doi.org/10.3390/w13192754

Academic Editors: Layla Ben Ayed, Eleni Golomazou, Panagiotis Karanis, Patrick Scheid, Ourania Tzoraki, Anna Lass and Muhammad Shahid Iqbal

Received: 9 September 2021
Accepted: 1 October 2021
Published: 4 October 2021

Abstract: This study aimed to assess, optimize and model the efficiencies of Fenton, photo-Fenton and ozonation/Fenton processes in formaldehyde elimination from water and wastewater using the response surface methodology (RSM) and artificial neural network (ANN). A sensitivity analysis was used to determine the importance of the independent variables. The influences of different variables, including H_2O_2 concentration, initial formaldehyde concentration, Fe dosage, pH, contact time, UV and ozonation, on formaldehyde removal efficiency were studied. The optimized Fenton process demonstrated 75% formaldehyde removal from water. The best performance with 80% formaldehyde removal from wastewater was achieved using the combined ozonation/Fenton process. The developed ANN model demonstrated better adequacy and goodness of fit with a R^2 of 0.9454 than the RSM model with a R^2 of 0. 9186. The sensitivity analysis showed pH as the most important factor (31%) affecting the Fenton process, followed by the H_2O_2 concentration (23%), Fe dosage (21%), contact time (14%) and formaldehyde concentration (12%). The findings demonstrated that these treatment processes and models are important tools for formaldehyde elimination from wastewater.

Keywords: formaldehyde removal; wastewater; photo-Fenton; ozonation; artificial neural network

1. Introduction

Water shortage and environmental problems are two of the most challenging topics in the world, which need more attention to tackle [1]. Formaldehyde is extensively used in different fields, such as wood processing; the chemical and petrochemical industries; the production of preservative, resin and textile industries and sterilizing and disinfection [2,3]. Furthermore, contaminated liquids with a high concentration of formaldehyde remain after the dehydrogenation or oxidation of methyl alcohol in various industries, which are discharged to the aquatic environment. The concentrations of formaldehyde in industrial effluents can vary from 100 to 10,000 mg/L [3,4]. Formaldehyde is a harmful compound and human carcinogen imposing damages on the environment and human health. According to the International Agency for Research on Cancer (IARC), formaldehyde has been classified as a group I carcinogenic substance for humans. Additionally, its teratogenic effect in both humans and animals has been established [5,6]. A threshold concentration

of 1.61-mg/L formaldehyde has been proposed for protecting the aquatic ecosystem [4]. Therefore, effluents containing formaldehyde must be treated before their discharge into the environment in order to protect aquatic ecosystems and human health.

Different processes have been used for the elimination of formaldehyde from wastewater, such as biological processes, adsorption, absorption, condensation, ion exchange and membrane technology [3,7]. However, each of these processes has certain limitations. For example, when investigating 100 mg/L of formaldehyde biodegradation by *Pseudomonas putida* IOFA1 in the concentrated effluents, formaldehyde cannot be adequately decomposed within 40 min [8]. In addition, formaldehyde reacts with the RNA and DNA of microorganisms, resulting in their deaths [4,8]. Advanced oxidation processes (AOPs) such as Fenton and photo-Fenton, which are based on the generation of one or more oxidants, have been identified as the most applicable processes for the degradation of recalcitrant chemical compounds [9,10]. Göde et al. [11] indicated that Fenton and Fenton-like processes can successfully treat landfill leachate. In addition, different investigations in photo-Fenton, photocatalysis and ozonation revealed the potentials of such processes in the successful elimination of recalcitrant compounds [12–14]. However, it has been reported that some recalcitrant compounds cannot be sufficiently decomposed with a single oxidant, and more and faster decompositions of the recalcitrant compounds have been reported with combined AOPs due to the simultaneous applications of various oxidants [15]. In the Fenton, photo-Fenton and ozonation/Fenton processes, various types of oxidants can be produced and applied for the decomposition of such contaminants [16,17]. Up to now, there has been a lack of studies comparing the performances of single and combined processes in formaldehyde removal from wastewater. Besides, to optimize such processes, researchers usually use different experimental procedures, which are time- and cost-consuming. Interestingly, the optimization and investigation of different conditions of the process can be aided by advanced study design and modeling procedures, which are rarely reported.

In order to determine the optimal conditions in a treatment system, the common approach is to keep all except one variable at an unspecified steady state [18–21]. The major disadvantage of such a single-parameter optimization procedure is its inability to detect the interactive effects of various independent variables on dependent variables and, hence, to generate correct net effects of these independent variables on the responses. The response surface methodology (RSM) is regarded as one of the most well-known methods in process design, modeling and optimization, as RSM can model the influences of various dependent variables both individually and through interactions on the responses. However, the obtained RSM model may not be sufficiently flexible to show the appropriate response surface [22].

In contrast to the traditional modeling methods, the artificial neural network (ANN) is an influential and powerful modeling method and demonstrates a great performance in modeling processes that are highly complicated without fully understanding their mechanisms [23]. Various researches have been reported regarding the application of both RSM and ANN modeling procedures. However, such modeling has not been reported regarding Fenton processes for formaldehyde removal [24]. In addition, the reported results showed that the performances of these models can be dependent on the type of phenomena that are being modeled [24,25]. Furthermore, a deep analysis will identify the relative importance of the variables affecting this process and help to improve the efficiency of the process, therefore addressing the deficiency and knowledge gap as well.

The objective of this study was to assess, compare and optimize the efficiencies of the Fenton, photo-Fenton and ozonation/Fenton processes in the elimination of formaldehyde from water and real wastewater from the adhesive manufacturing industry with respect to the effects of pH, contact time, initial concentration of formaldehyde, UV, dosage of Fe, H_2O_2 concentration and ozonation. In addition, RSM and ANN were employed to model and compare the Fenton process performance in formaldehyde elimination from wastewater. Furthermore, a sensitivity analysis was conducted to determine the relative

importance of the independent variables that are important to design more efficient studies in the future.

2. Materials and Methods

2.1. Materials

All of the chemicals, including formaldehyde, hydrochloric acid, sodium hydroxide, ethanol, ferric chloride, sodium sulfite, sulfuric acid, hydrogen peroxide and thymolphthalein, were of analytical grade and were provided by Merck, Germany. Wastewater was obtained from a wastewater treatment plant for the adhesive manufacturing industry, Mashhad, Iran. Stock solutions of formaldehyde and hydrogen peroxide were prepared by the dilution of 2.7 mL and 97.2 mL to 1 L, with a final concentration of 1000 mg/L and 1 mol/L, respectively. Ferric chloride and sodium sulfite solutions were prepared by dissolving 2.42 g and 126.043 g in distilled water and diluting up to 1 L, with a final concentration of 2420 mg/L and 1 mol/L, respectively. In order to prepare a solution for the determination of the consumed acid proportion, 1 g of thymolphthalein was dissolved in 1 L of methanol.

2.2. Experimental Procedure and Analysis

For the Fenton process, the experiments were carried out in a batch system using a cylindrical glass reactor of 250 mL. According to the designed runs by RSM, after pH adjustment and the addition of appropriate proportions of ferric chloride and hydrogen peroxide, the prepared samples containing formaldehyde were stirred during the contact times (15–90 min). Then, the samples were adjusted to pH $\geq$ 9 through the addition of a NaOH solution, from which 2-mL samples were filtered and titrated in 50 mL of sodium sulfite, using sulfuric acid with phenolphthalein as an indicator [26]. The formaldehyde proportion was calculated using Equation (1):

$$W = \left(\frac{[(V - B) \times M \times F]}{S} \right) \times 100 \quad (1)$$

where W is the weight of formaldehyde (%), V is the volume of H_2SO_4 for the sample titration (mL), B is the volume of H_2SO_4 for the blank titration (mL), M is the normality of H_2SO_4, F is 0.03003 (formaldehyde milliequivalent weight) and S is sample mass (g). After completing the experiments designed by the RSM for the Fenton process, the optimization of photo-Fenton and ozonation/Fenton were conducted. Finally, the optimized Fenton, photo-Fenton and ozonation/Fenton processes were applied to treat real industrial wastewater. For both the ozonation and photo-Fenton processes, the aforementioned reactor was applied, although a moveable UV lamp (40 W) covered in a quartz tube was horizontally installed on top of the reactor and completely covered with an aluminum foil in photo-Fenton process.

2.3. Experimental Design

A central composite design (CCD) as a standard RSM methodology was used to design the investigation procedure to model formaldehyde removal by Fenton process and determine the efficiency of the process. According to this procedure, the number of required experiments was calculated using Equation (2):

$$N = 2^n + 2n + n_c \quad (2)$$

where N is the number of required runs, n is the number of independent variables and n_c is the number of center points that are applied for assessing the experimental error and the data reproducibility [22]. Thus, for formaldehyde removal processes with five different independent variables (n = 5), including pH, contact time, initial concentration of

formaldehyde, Fe dosage and H_2O_2 concentration, as shown in Table 1, all of the considered runs were computed as Equation (3):

$$N = 2^n + 2n + n_c = 2^5 + 2(5) + 8 = 50 \quad (3)$$

Table 1. The independent variables, along with the levels of the independent variables, in the designed method.

Independent Factor	Coded Symbol	Range and Level				
		$-\alpha$	−1	0	+1	$+\alpha$
Fe dosage (mg/L)	A	20	28.69	35	41.31	50
Contact time (min)	B	2	36.19	61	85.81	120
Formaldehyde Concentration (mg/L)	C	100	215.91	300	384	500
pH	D	3	5.32	7	8.68	11
H_2O_2 (mol/L)	E	0.1	0.36	0.55	0.74	1

The dependent response variable was the efficiency of the formaldehyde removal using the three aforementioned processes. The calculation of the achieved experimental results was performed in accordance with the second-order polynomial Equation (4):

$$Y = \beta_0 + \sum_{i=1}^{n} \beta_i X_i + \sum_{i=1}^{n} \beta_{ii} X_i^2 + \sum_{i=1}^{n-1} \sum_{j=i+1}^{n} \beta_{ii} X_i X_j \quad (4)$$

In order to decrease the effects of uncontrolled parameters, all of the runs were replicated twice, and the sequences of the runs were randomized [22].

A Design Expert® 7.0 software program was applied to generate the quadratic model of the obtained experimental results, and the developed model was assessed using the analysis of variances (ANOVA). The determination coefficients (R^2, R^2_{adj}), along with the F-test, were used for the model goodness of fit and statistical significance assessments [22,27].

2.4. Optimization

The optimization of the Fenton process efficiency in the formaldehyde removal from water was carried out by the Design Expert® program. This program looks for a group of independent factor levels with the best efficiency in formaldehyde removal. During the optimization stage, each independent variable, including H_2O_2 concentration, initial concentration of formaldehyde, Fe dosage, contact time and pH, was chosen and optimized. Within the range, the maximum, minimum and none (only for the dependent parameters), coupled with setting an accurate value (only for the response factor), were the possible targets in this regard. Finally, an overall desirability was achieved from these possible targets. Additionally, after the optimization of the Fenton process parameters, the optimized Fe dosage, H_2O_2 concentration and initial formaldehyde concentration for Fenton were optimized in five different pH (3, 5, 7, 9 and 11) and four various contact times (15, 30, 60 and 90 min) with 20 experiments. In order to optimize the ozonation process, the same condition with a different contact time (15, 30, 60 and 80 min) was repeated in an ozone injection of 1.4 mg/(L min). It is worth mentioning that the formaldehyde concentration was 215.91 mg/L based on the Fenton optimization results. In addition, all the experiments were repeated to ensure the reproducibility of the results.

2.5. Formaldehyde Removal from Wastewater by FENTON, Photo-Fenton and Ozonation/Fenton Processes

The optimized Fenton, photo-Fenton and ozonation/Fenton processes were applied to treat real industrial wastewater from a wastewater treatment plant for adhesive manufacturing industry effluent located in Mashhad, Iran containing formaldehyde. During

the 24-h sampling period, 4-L samples were taken every 2 h from the influent of the treatment plant. After the formaldehyde analysis and sedimentation for 48 h, the efficiency of the Fenton, photo-Fenton and ozonation/Fenton processes in formaldehyde elimination were assessed.

2.6. Artificial Neural Network Modeling

A multilayer perceptron feedforward artificial neural network (MLP-FFANN) was applied to model the removal efficiency of formaldehyde from water by the Fenton process. Based on the proportions of the independent and dependent parameters, five and one nodes were used in the input and output layers to model the process, respectively. To obtain the best model, numerous proportions of nodes ranging from 1 to 20 were loaded in the hidden layer, and the performances of the built neural networks were evaluated using the mean squared error (MSE) in all the training, validation and test phases. The used training backpropagation algorithm for the development of the models was Levenberg-Marquardt. Additionally, the sigmoid transfer function (tansig) and linear transfer function (purelin) were used in the hidden and output layers, consecutively [23]. In order to model, 70%, 15% and 15% of the experimental results were allocated to the training, validation and test phases, respectively. In contrast to the output data, the experimental results were normalized in a range from 0.1 to 0.9 according to Equation (5) [23]:

$$\text{Normalized proportion of } x_i = \frac{x_i - \text{minimum proportion of data}}{\text{maximum proprtion of data} - \text{minimum proportion of data}} \times (0.9 - 0.1) + 0.1 \quad (5)$$

The reduction of the computational complexity, as well as prevention from overtraining, are two of the most important reasons for data normalization.

2.7. Comparison between RSM and ANN Models

In order to compare the models of the Fenton process, all of the experimental results were used to predict the formaldehyde removal efficiency by both the RSM and ANN models. Four different statistical parameters, including the root mean square error (RMSE), sum square error (SSE), Adjusted R^2 (Adj-R^2) and R^2, were calculated using the equations presented in Table 2 to evaluate the strengths of the developed models [28]. It is worth highlighting that higher proportions of the R^2, as well as Adjusted R^2 (Adj-R^2), along with lower proportions of the RMSE and SSE, principally demonstrated the model with a higher prediction strength.

Table 2. A summary of the equations of the error functions.

Index	Equation
Adjusted determination coefficient	$R^2 adjusted = 1 - \frac{(1-R^2)(N-1)}{N-p-1}$
Sum square error	$SSE = \sum_{i=1}^{N} \left(y_{prd,i} - y_{exp,i}\right)^2$
Determination coefficient	$R^2 = 1 - \frac{\sum_{i=1}^{N}\left(y_{prd,i} - y_{Act,i}\right)}{\sum_{i=1}^{N}\left(y_{prd,i} - y_m\right)}$
Root mean square error (RMSE)	$RMSE = \sqrt{\frac{1}{N}\sum_{i=1}^{N}\left(y_{prd,i} - y_{Act,i}\right)^2}$

y_m and N are the mean of the measured proportion of formaldehyde removal and the total number of data points, and $y_{Act,i}$ and $y_{pred,i}$ are the experimental and predicted proportions of formaldehyde removal.

2.8. Sensitivity Analysis

In order to assess the importance percentages of the independent variables in prediction of the response, Equation (6) was used.

$$Ij = \frac{\sum_{m=1}^{m=Nh}\left(\left(\frac{\left|W_{jm}^{ih}\right|}{\sum_{k=1}^{Ni}\left|W_{km}^{ih}\right|}\right)\times\left|W_{mn}^{ho}\right|\right)}{\sum_{k=1}^{k=Ni}\left\{\sum_{m=1}^{m=Nh}\left(\frac{\left|W_{km}^{ih}\right|}{\sum_{k=1}^{Ni}\left|W_{km}^{ih}\right|}\right)\times\left|W_{mn}^{ho}\right|\right\}}\times 100 \quad (6)$$

where I_j and N_i are the importance and the number of independent variables, consecutively; N_h, W, m, n and k are, correspondingly, the number of hidden layer nodes, ANN weight, the number of hidden nodes, the number of response factor (output) and the number of independent factors and i, h and o are, respectively, related to the input, hidden and output layers [29].

3. Results and Discussion

3.1. ANOVA and Assessment of Model Fitness

In order to determine the effects of five different independent variables on the formaldehyde elimination from water, fifty runs were designed and accomplished. The experimental results, coupled with the predicted results and the experimental conditions, are presented in Table 3.

At first, an empirical relationship was demonstrated between the coded independent variable and response factors by the fitted polynomial model. The fitted modified quadratic equation for the Fenton process is presented in Equation (7):

$$\begin{aligned} \mathrm{Y}(\%) = 59.46 - 4.14\ \mathrm{A} + 7.92\ \mathrm{B} - 4.91\ \mathrm{C} - 4.12\ \mathrm{D} - 7.97\ \mathrm{E}\ + 2.29\ \mathrm{AB} + 3.50\ \mathrm{BE} + 2.77\ \mathrm{CD} - 2.83\ \mathrm{CE} \\ -4.29\ \mathrm{A}^2 - 6.61\ \mathrm{B}^2 - 5.45\ \mathrm{E}^2 \end{aligned} \quad (7)$$

where Y is the efficiency of Fenton process in the elimination of formaldehyde, and A, B, C, D and E are the coded independent parameters demonstrated in Table 1. The validation and adequacy of the developed model were assessed using an ANOVA. Table 4 displays the significance of the coefficients, as well as the results of the ANOVA for the modified model. The F-test was applied to assess the goodness of fit of the model. According to the obtained output, the F-value was 77.34 for formaldehyde removal from water by the Fenton process. This demonstrated that the developed model for formaldehyde removal was significant (p-value < 0.05). The adequacy of the obtained model for formaldehyde removal was also assessed by a statistical factor (R^2), which was 0.9185, meaning that 8.15% of the variability in the formaldehyde removal efficiency was not described by the developed model. The calculated values of the predicted R^2 and Adj. R^2 for the Fenton process in the formaldehyde removal from water were 0.9186 and 0.9169, correspondingly, establishing the model's goodness-of-fit. Additionally, the differences between the proportions of the predicted R^2 and Adj. R^2 indicated that there was a good agreement between these two parameters in the developed model. In addition, the achieved Adeq Precision for this developed model was 23.46, demonstrating that there was a desired signal-to-noise ratio, which was higher than 4 [30]. Therefore, the obtained model was able to navigate in the designed spaces.

Table 3. The design matrix and the experimental vs. predicted results for the elimination of FA from aqueous solutions using the Fenton process.

	Actual Factor					Coded Factor					Real Efficiency (%)	RSM Prediction Efficiency (%)	ANN Prediction Efficiency (%)
	Fe Dosage (mg/L)	Contact Time (min)	Formaldehyde Concentration (mg/L)	pH	H_2O_2 Concentration (mol/L)	A (mg/L)	B (min)	C (mg/L)	D	E (mol/L)			
1	41.31	85.81	215.91	8.68	0.74	+1	+1	−1	+1	+1	50	45.56	49.92
2	41.31	36.19	215.91	5.32	0.74	+1	−1	−1	−1	+1	32.14	31.92	31.99
3	35	61	300	7	0.55	0	0	0	0	0	52.63	59.46	58.84
4	28.69	85.81	384.09	8.68	0.74	−1	+1	+1	+1	+1	41.66	39.32	41.62
5	28.69	85.81	384.09	5.32	0.36	−1	+1	+1	−1	−1	58.33	56.62	50.51
6	35	61	300	3	0.55	0	0	0	−2.38	0	81.57	69.26	81.12
7	35	61	100	7	0.55	0	0	−2.37	0	0	73.56	71.14	73.36
8	28.69	36.19	215.91	8.68	0.36	−1	−1	−1	+1	−1	50	48.28	49.86
9	28.69	85.81	384.09	5.32	0.74	−1	+1	+1	−1	+1	43.75	42.02	51.62
10	35	61	300	7	0.55	0	0	0	0	0	57.89	59.46	58.84
11	41.31	36.19	384.09	8.68	0.74	+1	−1	+1	+1	+1	6.25	8.2	9.31
12	35	61	300	7	0.55	0	0	0	0	0	58	59.46	58.84
13	35	120	300	7	0.55	0	+2.37	0	0	0	42.10	40.90	44.85
14	28.69	36.19	384.09	5.32	0.36	−1	−1	+1	−1	−1	54.16	52.36	48.96
15	35	61	300	7	0.10	0	0	0	0	−2.37	44.73	47.59	44.74
16	28.69	85.81	215.91	8.68	0.74	−1	+1	−1	+1	+1	53.57	49.26	53.40
17	41.31	36.19	215.91	8.68	0.36	+1	−1	−1	+1	−1	32.14	35.42	32.21
18	50	61	300	7	0.55	+2.37	0	0	0	0	31.57	25.34	31.50
19	41.31	85.81	384.09	5.32	0.36	+1	+1	+1	−1	−1	56.25	52.92	55.79
20	41.31	36.19	384.069	8.68	0.36	+1	−1	+1	+1	−1	41.66	36.8	41.62
21	35	61	300	7	1	0	0	0	0	+2.37	15.78	9.67	15.78
22	28.69	36.19	384.09	5.32	0.74	−1	−1	+1	−1	+1	29.16	23.76	29.14
23	41.31	36.19	384.09	5.32	0.74	+1	−1	+1	−1	+1	8.33	10.9	18.02
24	41.31	36.19	215.91	5.32	0.36	+1	−1	−1	−1	−1	53.57	49.2	66.78
25	35	61	300	7	0.55	0	0	0	0	0	57.89	59.46	58.84
26	41.31	85.81	384.09	5.32	0.74	+1	+1	+1	−1	+1	22.91	38.32	22.73
27	41.31	36.19	215.91	8.68	0.74	+1	−1	−1	+1	+1	14.28	18.14	10.12
28	35	61	300	7	0.55	0	0	0	0	0	57.89	59.46	58.84
29	28.69	85.81	384.09	8.68	0.36	−1	+1	+1	+1	−1	52.08	53.92	41.56
30	41.31	85.81	384.09	8.68	0.36	+1	+1	+1	+1	−1	50	50.22	49.60
31	28.69	85.81	215.91	5.32	0.74	−1	+1	−1	−1	+1	64.28	63.04	64.10
32	28.69	85.81	215.91	8.68	0.36	−1	+1	−1	+1	−1	57.14	52.54	57.04
33	28.69	36.19	384.09	8.68	0.74	−1	−1	+1	+1	+1	25	21.06	16.61
34	41.31	85.81	384.09	8.68	0.74	+1	+1	+1	+1	+1	33.33	35.62	33.24
35	41.31	85.81	215.91	5.32	0.36	+1	+1	−1	−1	−1	64.28	62.62	64.10

Table 3. *Cont.*

	Actual Factor					Coded Factor					Real Efficiency (%)	RSM Prediction Efficiency (%)	ANN Prediction Efficiency (%)
	Fe Dosage (mg/L)	Contact Time (min)	Formaldehyde Concentration (mg/L)	pH	H_2O_2 Concentration (mol/L)	A (mg/L)	B (min)	C (mg/L)	D	E (mol/L)			
36	20	61	300	7	0.55	−2.37	0	0	0	0	42.10	45.03	41.80
37	35	61	300	7	0.55	0	0	0	0	0	63.15	59.46	58.84
38	35	61	300	7	0.55	0	0	0	0	0	63.15	59.46	58.84
39	28.69	36.19	215.91	5.32	0.74	−1	−1	−1	−1	+1	42.85	44.78	42.67
40	28.69	36.19	215.91	5.32	0.36	−1	−1	−1	−1	−1	60.71	62.06	60.69
41	28.69	36.19	384.09	8.68	0.36	−1	−1	+1	+1	−1	50	49.66	49.93
42	28.69	85.81	215.91	5.32	0.36	−1	+1	−1	−1	−1	53.57	66.32	53.01
43	35	61	500	7	0.55	0	0	+2.37	0	0	48.48	47.78	48.46
44	41.31	85.81	215.91	8.68	0.36	+1	+1	−1	+1	−1	53.57	48.84	66.78
45	35	61	300	7	0.55	0	0	0	0	0	60.52	59.46	58.84
46	41.31	85.81	215.91	5.32	0.74	+1	+1	−1	−1	+1	53.57	59.34	53.01
47	35	2	300	7	0.55	0	−12.37	0	0	0	5.26	3.23	5.26
48	35	61	300	11	0.55	0	0	0	+2.37	0	47.36	49.66	47.25
49	41.31	36.19	384.09	5.32	0.36	+1	−1	+1	−1	−1	31.25	39.5	38.56
50	28.69	36.19	215.91	8.68	0.74	−1	−1	−1	+1	+1	21.42	31	16.65

Table 4. The results of the ANOVA, as well as the coefficient significance of the model parameters.

Source	ANOVA				
	Sum of Square	**df**	**Mean Square**	**F-Value**	***p*-Value**
Model	13,442.47	12	1120.21	34.77	<0.0001
A (Fe dosage)	741.43	1	741.43	23.01	<0.0001
B (Contact time)	2715.92	1	2715.92	84.3	<0.0001
C (FA con.)	1043.76	1	1043.76	32.4	<0.0001
D (pH)	734.72	1	734.72	22.8	<0.0001
E (H_2O_2 con.)	2748.62	1	2748.62	85.31	<0.0001
AB	167.51	1	167.51	5.2	0.0285
BE	391.32	1	391.32	12.15	0.0013
CD	245.81	1	245.81	7.63	0.0089
CE	255.82	1	255.82	7.94	0.0077
A^2	1052.81	1	1052.81	32.68	<0.0001
B^2	2505.84	1	2505.84	77.78	<0.0001
E^2	1701.79	1	1701.79	52.82	<0.0001
Residual	1192.1	37	32.22	-	-
Lack of fit	1110.06	30	37	3.16	0.0594
Pure error	82.04	7	11.72	-	-

3.2. Optimization of Different Fenton Processes in Formaldehyde Removal

Based on the experimental results from the Fenton process, the maximum formaldehyde removal was 75.0%. Further experiments were carried out to evaluate the validity of the developed RSM model and optimized condition. The proposed optimum conditions for the pH, initial concentration of formaldehyde, Fe dosage, H_2O_2 concentration and contact time were 5.32, 215.91 mg/L, 33.9 mg/L, 0.5 mol/L and 72 min, under which, the estimated formaldehyde removal efficiency was 73.8%. This value was very close to the experimentally derived removal of 75% obtained under the optimum condition.

On the basis of the optimized Fenton conditions, the effect of UV alone on formaldehyde removal during the photo-Fenton process was assessed at 215.91 mg/L of formaldehyde; various pH (3–11) and at four contact times (15 min, 30 min, 60 min and 90 min). As shown in Table 5. the highest removal efficiency was 14.3% at pH 5 and a contact time of 90 min. Regarding the fact that the optimum contact time was achieved in 72 min for the Fenton process, in order to investigate the possibility of this 18-min difference in time, the removal efficiency was evaluated at pH 5 in 15 min, 30 min, 60 min and 80 min. As shown in Figure 1a, the experimental results for the formaldehyde elimination efficiency were 5.0%, 7.1%, 9.3% and 12.0%, respectively. Thus, the optimized conditions were selected as pH 5 and a contact time of 80 min, based on the formaldehyde treatment efficiency.

Table 5. The experimental results of the photo-Fenton process optimization for formaldehyde removal (%).

pH	Time (min)			
	15	**30**	**60**	**90**
3	0	3.57	7.14	9.28
5	3.57	7.14	9.28	14.25
7	2.1	3.57	6.42	7.14
9	5	7.14	10.71	10.71
11	0	3.57	7.14	9.28

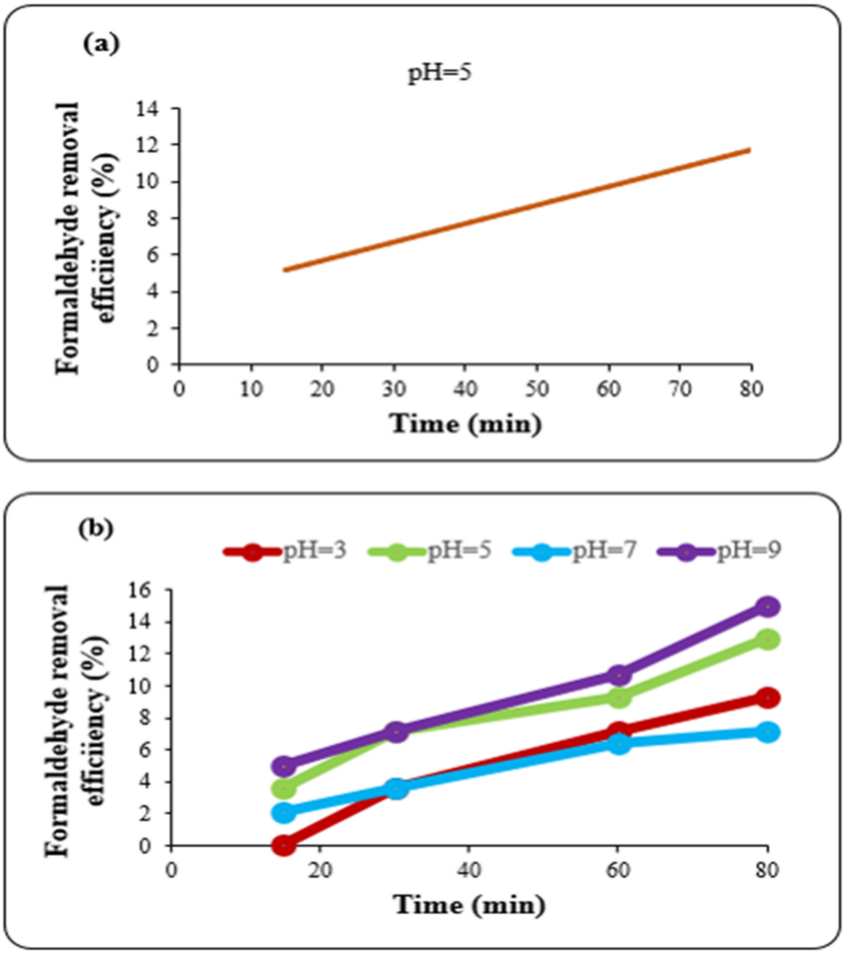

Figure 1. (**a**) Effect of photo-Fenton on the formaldehyde removal at pH 5. (**b**) The results of ozonation in the formaldehyde removal at different pH and contact times. Ozone concentration = 1.4 mg/L min; formaldehyde concentration = 215.91 mg/L.

During the ozonation/Fenton treatment, the influence of ozonation on formaldehyde removal from water was investigated under the previously optimized Fenton conditions for the Fe dosage; H_2O_2 concentration and initial concentration of formaldehyde at various contact times (15 min, 30 min, 60 min and 80 min) with different pH (3, 5, 7, 9 and 11). The results (Figure 1b) showed that ozonation alone had the best efficiency of 15.0% removal at pH 9 and a contact time of 80 min.

Based on the chemical analysis, the formaldehyde concentration in real wastewater samples was 375 mg/L. Following wastewater treatment under the optimized Fenton, photo-Fenton and ozonation/Fenton processes, the formaldehyde removal was found to be 60%, 72% and 80%, respectively. The results therefore showed that the ozonation/Fenton process demonstrated the best performance in formaldehyde removal from real industrial wastewater.

3.3. Effects of Variables on Formaldehyde Removal

With respect to the obtained model, the mentioned intercept proportion (58.56%) that was gained for formaldehyde removal was not dependent on the independent factors or their quadratic and interaction terms. In the statistical analysis, the parameters E (H_2O_2 concentration) and B (contact time) were regarded as the most important factors, with coefficients of −7.97 and +7.92, respectively (Equation (7)). After these two parameters, the other significant parameters influencing the formaldehyde elimination in decreasing order were the quadratic contact time and quadratic H_2O_2 concentration, concentration of formaldehyde, quadratic Fe dosage, Fe dosage, solution pH, interaction between the

contact time and H_2O_2 concentration, interaction between the formaldehyde concentration and H_2O_2 concentration, interaction between the formaldehyde concentration and pH and interaction between the Fe dosage and contact time.

3.3.1. Effects of H_2O_2 Concentration

As shown in Equation (7), there was an inverse relationship between the initial concentration of H_2O_2 (E) and removal efficiency (Y), with a coefficient of −7.97. When the concentration of H_2O_2 was increased from 0.36 to 0.74 mol/L, the formaldehyde removal efficiency decreased from 60.1% to 7.7%. This can be due to the fact that, in higher concentrations of H_2O_2, some oxidants with lower oxidation power can be generated [31]. In addition, Evgenidou et al. [32] reported that high concentrations of H_2O_2 demonstrated an inhibitory effect on degradation owing to its plausible scavenger function for free radicals. However, lower concentrations of H_2O_2 can result in a lower production of active radicals and, consequently, a slower rate of oxidation [31]. It is worth highlighting that, in agreement with the obtained results, there have been many studies in which the effect of H_2O_2 on the degradation of pollutants followed the same pattern [33,34]. Similarly, it has been reported that there is a strong dependence between H_2O_2 and ferrous ions during pollutant degradation [35].

3.3.2. Effects of Contact Time

According to Equation (7) and Figure 2a, the higher the contact time, the greater the removal efficiency of formaldehyde was obtained after 120 min. The results can be due to the fact that the production of active species from H_2O_2 decomposition increased with the contact time, increasing the interactions between the pollutant molecules with active species occurring. Based on the results and cost implications, a contact time of 72 min was chosen as the optimum. Similarly, an experimental duration of 60 min was proposed for formaldehyde decomposition in other studies [35,36]. In contrast to other AOPs, the production of radicals in the Fenton process occurs with high concentrations during the first few minutes; hence, a duration of 72 min is appropriate for both radical production and cost minimization [37].

3.3.3. Effects of Initial Formaldehyde Concentration

With respect to the stoichiometric aspect for decomposition, it is of great significance to consider the ratio of oxidant to contaminant in order to ensure sufficient active species for formaldehyde. As the formaldehyde concentration may affect the Fenton process efficiency, it was examined in a range from 100 to 500 mg/L. As shown in Figure 2a and Equation (7), there was an inverse linear relationship between the initial formaldehyde concentration (C) and formaldehyde elimination efficiency (Y). This relationship is likely due to the number of active species, particularly hydroxyl radicals per formaldehyde molecule, which become smaller with the increasing formaldehyde concentration. This also explains the negative relationship between formaldehyde and H_2O_2 concentrations [38].

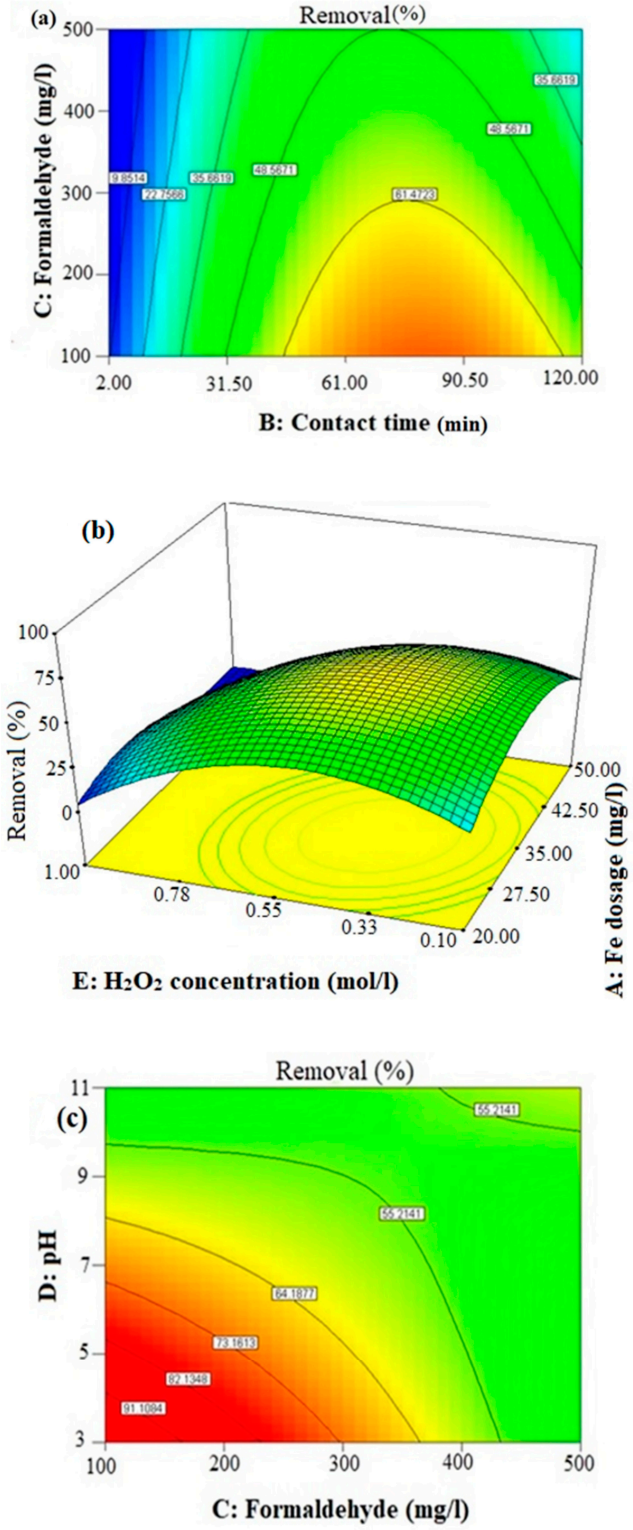

Figure 2. The combined effects of (**a**) the formaldehyde concentration and contact time, (**b**) Fe dosage and H_2O_2 concentration and (**c**) pH and initial formaldehyde concentration on the elimination of formaldehyde from wastewater in the Fenton process.

3.3.4. Effects of Fe Dosage

According to Figure 2b, the efficiency of the Fenton process in formaldehyde removal increased with the Fe concentrations (up to 35 mg/L), then decreased with a further increase to 50 mg/L of Fe. Regarding the other performed studies, Fe, especially its ferrous

form, is so important for the adequate production of hydroxyl radicals, suggesting a direct relationship between the Fe dosage and production of hydroxyl radicals. Similarly, these explanations can justify the interactive positive effects of the Fe dosage and contact time [39,40]. In another study by Kitis and Kapalan [41], the inhibitory function of higher Fe concentrations to generate free radicals was demonstrated; therefore, its downward trend may also result from a scavenger function of Fe for the formation of free radicals. The results in another study demonstrated that the effect of zero-valent iron on dye removal by the Fenton process was not significant, which can be explained by the different interactions among Fe and other active species under different conditions [41,42].

3.3.5. Effects of pH

The solution pH is regarded as one of the most important factors affecting the Fenton process efficiency. As shown in Figure 2c, there was an inverse relationship between the pH and formaldehyde removal in the Fenton process, due to the reaction of $^{\cdot}OH$ with Fe and precipitation of iron in alkaline conditions [43]. Another reason for this may be attributed to the hydrolysis of hydrogen peroxide into H_2O and O_2 at an alkaline pH. Moreover, the formation of carbonates produced in alkaline pH may be another plausible reason, which can deactivate the hydroxyl radicals [44].

3.3.6. Effects of UV

As demonstrated in Figure 1a, the UV alone can eliminate formaldehyde from water up to 12% in 80 min. UV is able to photolyze both Fe(III)-peroxo complexes and ferric ions to ferrous ions (Fe^{2+}), which are more effective than Fe^{3+} for hydroxyl radical generation, and directly produce hydroxyl radicals from the mentioned compound. Therefore, UV can increase the production of active species and, consequently, formaldehyde oxidation. Equations (8)–(10) show the related reactions for the formation of free radicals [17,45–47]:

$$Fe^{2+} + H_2O_2 \rightarrow Fe^{3+} + OH^- + {}^{\bullet}OH \quad (8)$$

$$Fe(OH)^{2+} + h\vartheta \rightarrow Fe^{2+} + {}^{\bullet}OH \quad (9)$$

$$H_2O_2 + h\vartheta \rightarrow 2{}^{\bullet}OH \quad (10)$$

3.3.7. Effects of pH on Formaldehyde Removal in Ozonation Process

According to Figure 1b, there is a direct relationship between the formaldehyde removal efficiency and pH value. As ozone reacts with pollutants in two ways, including direct oxidation occurring in acidic conditions and indirect oxidation at which hydroxyl radicals generated from ozone hydrolysis oxidize the pollutant. Ozone hydrolysis is completely dependent upon the pH, and there is a direct relationship between these two parameters. Ozone can be easily hydrolyzed in alkaline conditions, because hydroxyl ions, being primers of hydroxyl radical formation and ozone hydrolysis reactions, are abundant in alkaline conditions. The generation of hydroxyl radicals from ozone is carried out as shown in Equations (11) and (12) [48]:

$$O_3 + OH^- \rightarrow HO_2^- + O_2 \quad (11)$$

$$O_3 + HO_2^- \rightarrow {}^{\bullet}OH + O_2^- + O_2 \quad (12)$$

Therefore, from the above discussion and higher oxidation potential of hydroxyl radicals than ozone, the better efficiency of the ozonation process in formaldehyde removal can be justified in agreement with other studies [16].

3.4. Artificial Neural Network

According to the results for the Fenton process, a model with a topology of 5–7–1 was the best model. The prediction of the ANN model for formaldehyde removal efficiency by the Fenton process was obtained from Equation (13). The predicted proportions of the

formaldehyde removal vs. the experimental ones are depicted by Figure 3, showing the *R* proportions of the developed models in the training (0.9952), validation (0.9359) and test (0.9592) phases.

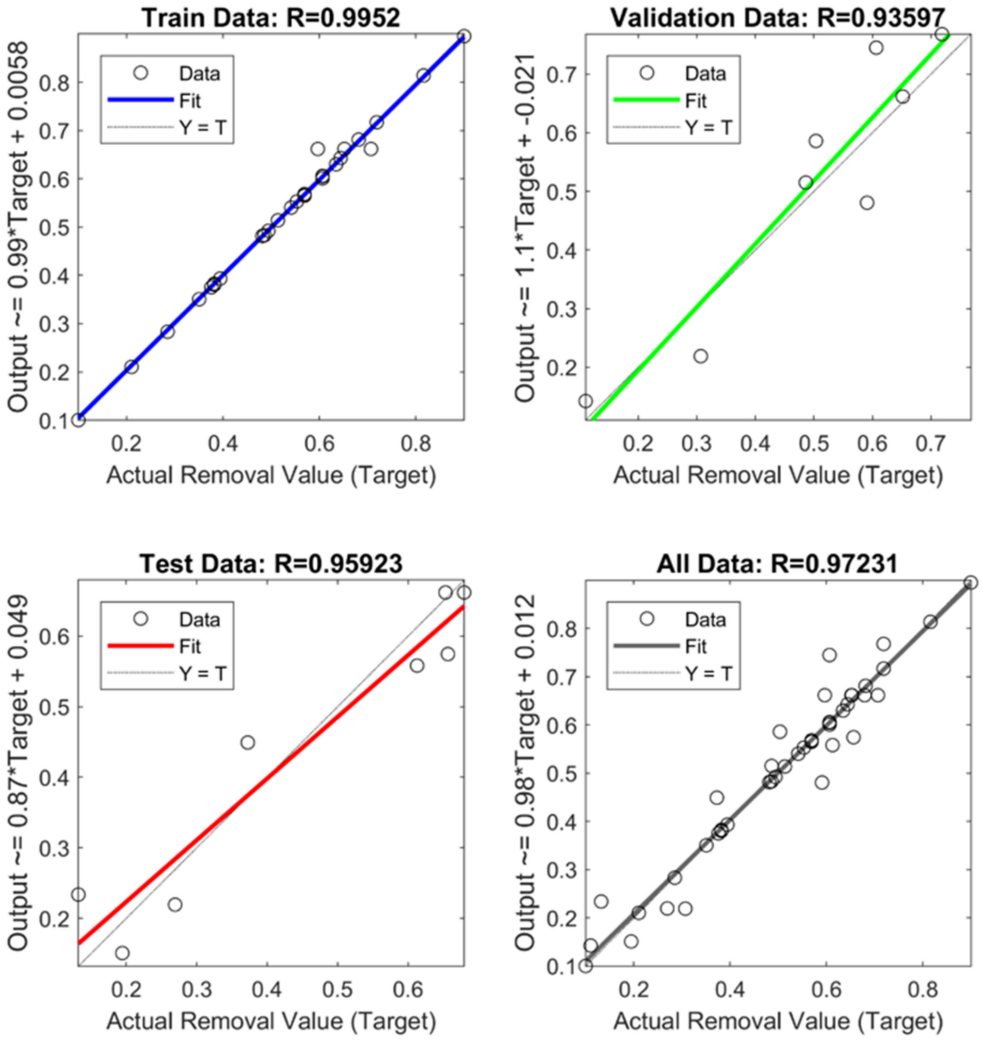

Figure 3. Scatter plots of the predicted and actual formaldehyde removal efficiencies in all the phases.

$$\text{ANN} = \text{purelin}\left\{W2 \times \text{tansig}\left(W1 \times [\text{Fe dosage}; \text{Contact time}; \text{Initial concentration of FA}; \text{pH}; H_2O_2] + b_1\right) + b_2\right\} \quad (13)$$

where W1, W2, b_1 and b_2 are the connection weights of the output and hidden layers and the biases of the hidden and output layers, consecutively. The obtained connection weights are listed in Table 6.

Table 6. The gained weights of the developed ANN models for formaldehyde removal from aqueous solutions by the Fenton process.

W1					W2	b_1	b_2
H_2O_2 Concentration	pH	Formaldehyde Concentration	Contact Time	Fe Dosage			
1.530	−0.784	0.084	2.620	2.464	−1.236	−3.302	
−0.215	−0.571	1.716	1.206	0.127	0.016	1.460	
2.437	0.628	−0.716	−3.037	0.461	−0.58	−1.447	
0.894	−1.803	−0.377	0.034	1.261	−0.112	1.291	1.799
0.298	1.165	1.455	−1.065	0.527	−0.847	0.453	
0.380	0.523	0.818	−1.695	1.904	0.652	1.177	
2.343	0.948	0.878	0.438	−0.598	0.388	1.549	

The best linear fit together with the R^2 of the constructed model is presented in Equations (14) and (15):

$$y = 0.9774x + 1.0876 \quad (14)$$

$$R^2 = 0.9454 \quad (15)$$

where x and y are the actual and predicted values of the formaldehyde removal.

Figure 4 depicts the residual errors distribution and the predicted proportions of the response variable by the developed RSM and ANN models. The results showed that the prediction strength of the ANN model was better than the RSM model.

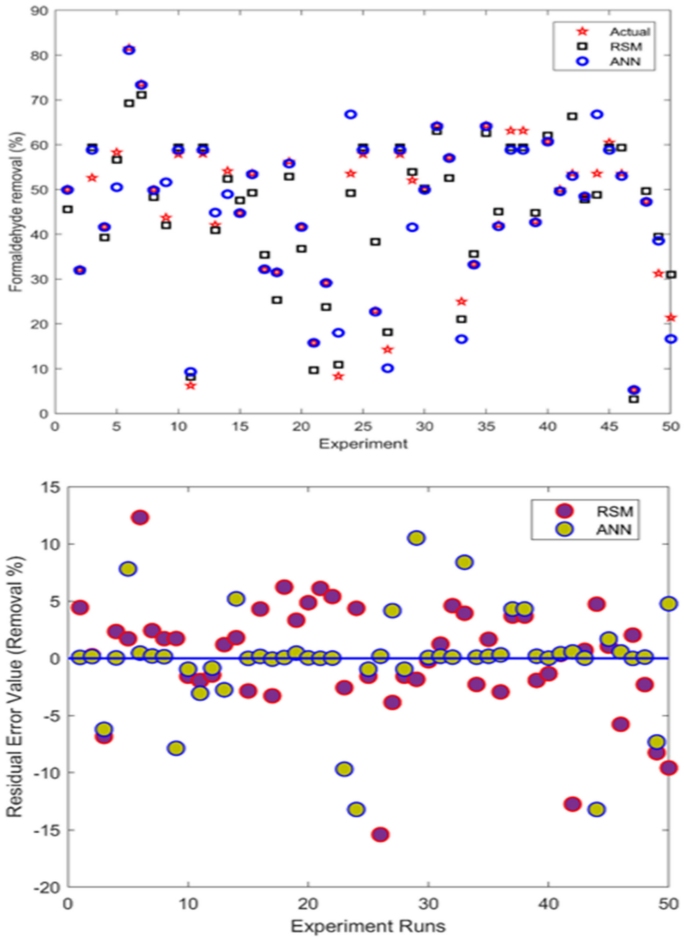

Figure 4. Comparison of the residual errors, along with the actual and predicted values of the formaldehyde removal efficiency by the ANN and RSM models.

3.5. Comparison between the RSM and ANN Models

In order to compare the performances of these two models in the prediction of formaldehyde removal from water by the Fenton process, four statistical indexes, including the RMSE, SSE, R-squared and adj-R^2, were used. The RMSE and SSE showed the errors of the models' predictions in two different ways, and the R-squared and adj-R^2 show the strengths and goodness of fit of the models in two different ways, which can be seen in detail in Table 2. The obtained results for the mentioned indexes are presented in Table 7. In addition, the predicted values of the response variables by the RSM and ANN models coupled with the actual ones are listed in Table 3. According to the results for the statistical indices, the ANN model showed a higher R^2 (0.9454) and Adj-R^2 (0.9443) and a lower RMSE (4.03) and SSE (8.15) than those of the RSM model, with 0.9186, 0.9169, 4.882 and 11.91, respectively. Therefore, the ANN can predict the process efficiency slightly better than the RSM.

Table 7. Comparison of the ANN and RSM model adequacies for formaldehyde removal by the Fenton process.

Statistical Index	ANN	RSM
SSE	8.15	11.91
RMSE	4.03	4.882
R^2	0.9454	0.9186
Adj-R^2	0.9443	0.9169

3.6. Sensitivity Analysis

The effective portions (%) of the dependent variables, including the Fe dosage, contact time, pH, H_2O_2 and initial concentration of formaldehyde in the Fenton process, were evaluated. The obtained connection weights for the built model presented in Table 6 were applied by this method. Figure 5 depicts the importance of the independent variables. As can be observed, the solution pH was ranked as the most critical factor with 31% importance, followed by the H_2O_2 concentration (23%), Fe dosage (21%), contact time (14%) and initial formaldehyde concentration (12%).

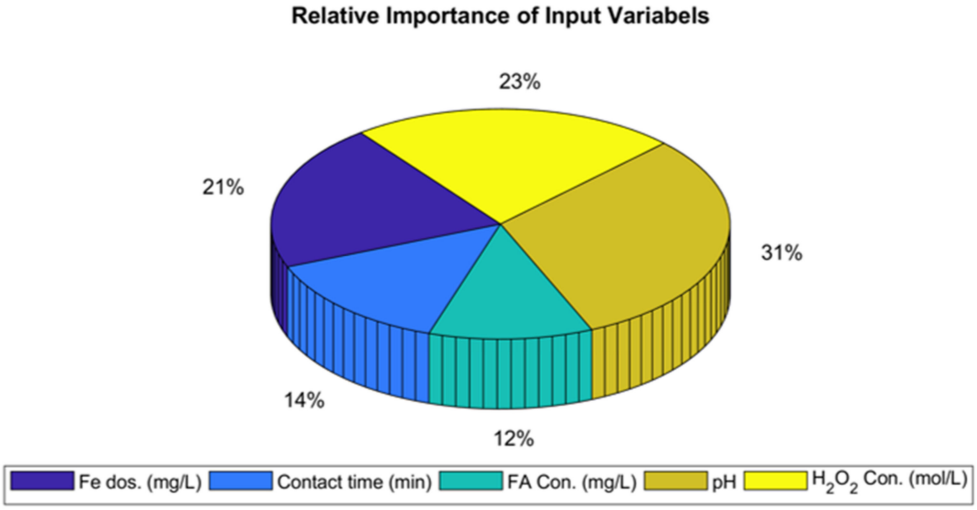

Figure 5. Importance percentages of the independent factors (Fe dosage, contact time, formaldehyde concentration, pH and H_2O_2 concentration) affecting the formaldehyde removal during the Fenton process.

4. Conclusions

This study assessed and optimized the performances of the Fenton, photo-Fenton and ozonation/Fenton processes in formaldehyde removal from water and wastewater with respect to the effects of the pH, formaldehyde concentration, contact time, H_2O_2 concentration, Fe dosage and UV. The maximum formaldehyde removal efficiency of 73.8% was obtained during the Fenton process under the optimum conditions of a pH of 5.32, initial concentration of formaldehyde of 215.91 mg/L, Fe dosage of 33.9 mg/L, H_2O_2 concentration of 0.5 mol/L and contact time of 72 min. Regarding the effect of UV, the highest formaldehyde removal was 14.3% under a pH of 5 and contact time of 90 min. With respect to the ozonation, a formaldehyde removal of 15% was achieved under a pH of 9 and contact time of 60 min. Finally, the performances of the optimized Fenton, photo-Fenton and ozonation/Fenton processes in a real wastewater treatment containing 375-mg/L formaldehyde were 60.0%, 72.0% and 80.0%, correspondingly. Moreover, the comparison of the RSM and ANN models' strengths in the prediction of the process efficiency for formaldehyde removal and the sensitivity analysis were accomplished. The sensitivity analysis showed that the most important factor affecting formaldehyde removal by the Fenton process was the pH, followed by the H_2O_2 concentration, Fe dosage, contact time and formaldehyde

initial concentration in decreasing order. In addition, the combined ozonation/Fenton process was identified as the best one for a formaldehyde removal efficiency of 80.0% from real wastewater, followed by photo-Fenton (72.0%) and Fenton (60.0%). Therefore, the ozonation/Fenton process is recommended for industrial wastewater treatment in the removal of formaldehyde and similar carcinogenic compounds.

Author Contributions: Conceptualization, A.A.N. (Ali Asghar Najafpoor) and A.A.N. (Ali Asghar Navaei); methodology A.A.N (Ali Asghar Navaei) and A.H.; A.D. software, A.H. and M.Y.; validation, A.A.N. (Ali Asghar Najafpoor), N.R. and J.L.Z.; formal analysis, A.H., A.A.N. (Ali Asghar Navaei) and T.B.; investigation, A.A.N. (Ali Asghar Navaei) and A.H.; resources, A.A.N. (Ali Asghar Najafpoor); data curation, A.A. and T.B.; writing—original draft preparation, A.H.; writing—review and editing, A.H., J.L.Z. and A.A.; visualization, A.A.N. (Ali Asghar Navaei); supervision, A.A.N. (Ali Asghar Najafpoor), J.LZ., N.R. and A.D.; project administration, A.A.N. (Ali Asghar Najafpoor) and funding acquisition, A.A.N. (Ali Asghar Najafpoor). All authors have read and agreed to the published version of the manuscript.

Funding: This research was funded by the Mashhad University of Medical Sciences (MUMS). In addition, the University of Technology Sydney has provided an International Research Scholarship and UTS President's Scholarship.

Institutional Review Board Statement: Not applicable.

Informed Consent Statement: Not applicable.

Data Availability Statement: The obtained data has been shared in the article.

Conflicts of Interest: The authors declare no conflict of interest.

References

1. Hosseinzadeh, A.; Zhou, J.L.; Navidpour, A.H.; Altaee, A. Progress in osmotic membrane bioreactors research: Contaminant removal, microbial community and bioenergy production in wastewater. *Bioresour. Technol.* **2021**, *330*, 124998. [CrossRef] [PubMed]
2. Abbaszadeh Haddad, F.; Moussavi, G.; Moradi, M. Advanced oxidation of formaldehyde in aqueous solution using the chemicalless UVC/VUV process: Kinetics and mechanism evaluation. *J. Water Process Eng.* **2019**, *27*, 120–125. [CrossRef]
3. Mei, X.; Guo, Z.; Liu, J.; Bi, S.; Li, P.; Wang, Y.; Shen, W.; Yang, Y.; Wang, Y.; Xiao, Y.; et al. Treatment of formaldehyde wastewater by a membrane-aerated biofilm reactor (MABR): The degradation of formaldehyde in the presence of the cosubstrate methanol. *Chem. Eng. J.* **2019**, *372*, 673–683. [CrossRef]
4. Guimarães, J.R.; Turato Farah, C.R.; Maniero, M.G.; Fadini, P.S. Degradation of formaldehyde by advanced oxidation processes. *J. Environ. Manag.* **2012**, *107*, 96–101. [CrossRef]
5. Reingruber, H.; Pontel, L.B. Formaldehyde metabolism and its impact on human health. *Curr. Opin. Toxicol.* **2018**, *9*, 28–34. [CrossRef]
6. Morshedi Rad, D.; Alsadat Rad, M.; Razavi Bazaz, S.; Kashaninejad, N.; Jin, D.; Ebrahimi Warkiani, M. Intracellular Delivery: A Comprehensive Review on Intracellular Delivery. *Adv. Mater.* **2021**, *33*, 2170103. [CrossRef]
7. Suresh, S.; Bandosz, T.J. Removal of formaldehyde on carbon -based materials: A review of the recent approaches and findings. *Carbon* **2018**, *137*, 207–221. [CrossRef]
8. Jin, M.; Yu, X.; Chen, X.; Zeng, R. Pseudomonas putida IOFA1 transcriptome profiling reveals a metabolic pathway involved in formaldehyde degradation. *Process Biochem.* **2016**, *51*, 220–228. [CrossRef]
9. Bao, T.; Damtie, M.M.; Wei, W.; Phong Vo, H.N.; Nguyen, K.H.; Hosseinzadeh, A.; Cho, K.; Yu, Z.M.; Jin, J.; Wei, X.L.; et al. Simultaneous adsorption and degradation of bisphenol A on magnetic illite clay composite: Eco-friendly preparation, characterizations, and catalytic mechanism. *J. Clean. Prod.* **2020**, *287*, 125068. [CrossRef]
10. Kamranifar, M.; Al-Musawi, T.J.; Amarzadeh, M.; Hosseinzadeh, A.; Nasseh, N.; Qutob, M.; Arghavan, F.S. Quick adsorption followed by lengthy photodegradation using FeNi3@SiO2@ZnO: A promising method for complete removal of penicillin G from wastewater. *J. Water Process. Eng.* **2021**, *40*, 101940. [CrossRef]
11. Göde, J.N.; Hoefling Souza, D.; Trevisan, V.; Skoronski, E. Application of the Fenton and Fenton-like processes in the landfill leachate tertiary treatment. *J. Environ. Chem. Eng.* **2019**, *7*, 103352. [CrossRef]
12. Bansal, P.; Verma, A. Pilot-scale single-step reactor combining photocatalysis and photo-Fenton aiming at faster removal of Cephalexin. *J. Clean. Prod.* **2018**, *195*, 540–551. [CrossRef]
13. Zakeri, H.; Yousefi, M.; Mohammadi, A.; Baziar, M.; Mojiri, S.; Salehnia, S.; Hosseinzadeh, A. Chemical coagulation-electro fenton as a superior combination process for treatment of dairy wastewater: Performance and modelling. *Int. J. Environ. Sci. Technol.* **2021**. [CrossRef]

14. Xu, B.; Ahmed, M.B.; Zhou, J.L.; Altaee, A.; Xu, G.; Wu, M. Graphitic carbon nitride based nanocomposites for the photocatalysis of organic contaminants under visible irradiation: Progress, limitations and future directions. *Sci. Total Environ.* **2018**, *633*, 546–559. [CrossRef]
15. Monteagudo, J.M.; Carmona, M.; Durán, A. Photo-Fenton-assisted ozonation of p-Coumaric acid in aqueous solution. *Chemosphere* **2005**, *60*, 1103–1110. [CrossRef] [PubMed]
16. Zheng, S.; Cui, C.; Liang, Q.; Xia, X.; Yang, F. Ozonation performance of WWTP secondary effluent of antibiotic manufacturing wastewater. *Chemosphere* **2010**, *81*, 1159–1163. [CrossRef]
17. López-Vinent, N.; Cruz-Alcalde, A.; Romero, L.E.; Chávez, M.E.; Marco, P.; Giménez, J.; Esplugas, S. Synergies, radiation and kinetics in photo-Fenton process with UVA-LEDs. *J. Hazard. Mater.* **2019**, *380*, 120882. [CrossRef]
18. Kardani, R.; Asghari, M.; Hamedani, N.F.; Afsari, M. Mesoporous copper zinc bimetallic imidazolate MOF as nanofiller to improve gas separation performance of PEBA-based membranes. *J. Ind. Eng. Chem.* **2020**, *83*, 100–110. [CrossRef]
19. Afsari, M.; Asghari, M.; Mohammadi Moghaddam, P. Synthesis and characterization of supported Phenolic resin/Carbon nanotubes Carbon membranes for gas separation. *Int. J. Nano Dimens.* **2017**, *8*, 316–328.
20. Najafpoor, A.A.; Dousti, S.; Joneidi Jafari, A.; Hosseinzadeh, A. Efficiency in phenol removal from aqueous solutions of pomegranate peel ash as a natural adsorbent. *Environ. Health Eng. Manag.* **2016**, *3*, 41–46.
21. Rezaei, M.; Radfar, P.; Winter, M.; McClements, L.; Thierry, B.; Warkiani, M.E. Simple-to-Operate Approach for Single Cell Analysis Using a Hydrophobic Surface and Nanosized Droplets. *Anal. Chem.* **2021**, *93*, 4584–4592. [CrossRef]
22. Najafpoor, A.A.; Jafari, A.J.; Hosseinzadeh, A.; Jazani, R.K.; Bargozin, H. Optimization of non-thermal plasma efficiency in the simultaneous elimination of benzene, toluene, ethyl-benzene, and xylene from polluted airstreams using response surface methodology. *Environ. Sci. Pollut. Res.* **2018**, *25*, 233–241. [CrossRef]
23. Almuntashiri, A.; Hosseinzadeh, A.; Volpin, F.; Ali, S.M.; Dorji, U.; Shon, H.; Phuntsho, S. Removal of pharmaceuticals from nitrified urine. *Chemosphere* **2021**, *280*, 130870. [CrossRef] [PubMed]
24. Chamoli, S. ANN and RSM approach for modeling and optimization of designing parameters for a V down perforated baffle roughened rectangular channel. *Alex. Eng. J.* **2015**, *54*, 429–446. [CrossRef]
25. Mohammadinia, A.; Saeidian, B.; Pradhan, B.; Ghaemi, Z. Prediction mapping of human leptospirosis using ANN, GWR, SVM and GLM approaches. *BMC Infect. Dis.* **2019**, *19*, 1–18. [CrossRef] [PubMed]
26. American Society for Testing and Materials (ASTM) International. *Standard Test Method for Concentration of Formaldehyde Solutions*; ASTM: West Conshohocken, PA, USA, 2012.
27. Najafpoor, A.A.; Sadeghi, A.; Alidadi, H.; Davoudi, M.; Mohebrad, B.; Hosseinzadeh, A.; Jafarpour, S.; Zarei, A. Biodegradation of high concentrations of phenol by baker's yeast in anaerobic sequencing batch reactor. *Environ. Health Eng. Manag.* **2015**, *2*, 79–86.
28. Baziar, M.; Nabizadeh, R.; Mahvi, A.H.; Alimohammadi, M.; Naddafi, K.; Mesdaghinia, A.; Aslani, H. Effect of dissolved oxygen/nZVI/persulfate process on the elimination of 4-chlorophenol from aqueous solution: Modeling and optimization study. *Korean J. Chem. Eng.* **2018**, *35*, 1128–1136. [CrossRef]
29. Baziar, M.; Azari, A.; Karimaei, M.; Gupta, V.K.; Agarwal, S.; Sharafi, K.; Maroosi, M.; Shariatifar, N.; Dobaradaran, S. MWCNT-Fe3O4 as a superior adsorbent for microcystins LR removal: Investigation on the magnetic adsorption separation, artificial neural network modeling, and genetic algorithm optimization. *J. Mol. Liq.* **2017**, *241*, 102–113. [CrossRef]
30. Hemmat Esfe, M.; Rostamian, H.; Shabani-samghabadi, A.; Abbasian Arani, A.A. Application of three-level general factorial design approach for thermal conductivity of MgO/water nanofluids. *Appl. Therm. Eng.* **2017**, *127*, 1194–1199. [CrossRef]
31. Suh, J.H.; Mohseni, M. A study on the relationship between biodegradability enhancement and oxidation of 1,4-dioxane using ozone and hydrogen peroxide. *Water Res.* **2004**, *38*, 2596–2604. [CrossRef]
32. Evgenidou, E.; Fytianos, K.; Poulios, I. Photocatalytic oxidation of dimethoate in aqueous solutions. *J. Photochem. Photobiol. A.* **2005**, *175*, 29–38. [CrossRef]
33. Matira, E.M.; Chen, T.-C.; Lu, M.-C.; Dalida, M.L.P. Degradation of dimethyl sulfoxide through fluidized-bed Fenton process. *J. Hazard. Mater.* **2015**, *300*, 218–226. [CrossRef]
34. Mohammadifard, Z.; Saboori, R.; Mirbagheri, N.S.; Sabbaghi, S. Heterogeneous photo-Fenton degradation of formaldehyde using MIL-100(Fe) under visible light irradiation. *Environ. Pollut.* **2019**, *251*, 783–791. [CrossRef]
35. Cetinkaya, S.G.; Morcali, M.H.; Akarsu, S.; Ziba, C.A.; Dolaz, M. Comparison of classic Fenton with ultrasound Fenton processes on industrial textile wastewater. *Sustain. Environ. Res.* **2018**, *28*, 165–170. [CrossRef]
36. Bandala, E.R.; Peláez, M.A.; Salgado, M.J.; Torres, L. Degradation of sodium dodecyl sulphate in water using solar driven Fenton-like advanced oxidation processes. *J. Hazard. Mater.* **2008**, *151*, 578–584. [CrossRef] [PubMed]
37. Zorpas, A.A.; Costa, C.N. Combination of Fenton oxidation and composting for the treatment of the olive solid residue and the olive mile wastewater from the olive oil industry in Cyprus. *Bioresour. Technol.* **2010**, *101*, 7984–7987. [CrossRef] [PubMed]
38. Benitez, F.J.; Beltran-Heredia, J.; Acero, J.L.; Rubio, F.J. Oxidation of several chlorophenolic derivatives by UV irradiation and hydroxyl radicals. *J. Chem. Technol. Biotechnol.* **2001**, *76*, 312–320. [CrossRef]
39. Kang, Y.W.; Hwang, K.-Y. Effects of reaction conditions on the oxidation efficiency in the Fenton process. *Water Res.* **2000**, *34*, 2786–2790. [CrossRef]
40. Goslan, E.H.; Gurses, F.; Banks, J.; Parsons, S.A. An investigation into reservoir NOM reduction by UV photolysis and advanced oxidation processes. *Chemosphere* **2006**, *65*, 1113–1119. [CrossRef]

41. Kitis, M.; Kaplan, S.S. Advanced oxidation of natural organic matter using hydrogen peroxide and iron-coated pumice particles. *Chemosphere* **2007**, *68*, 1846–1853. [CrossRef]
42. Hou, M.-F.; Liao, L.; Zhang, W.-D.; Tang, X.-Y.; Wan, H.-F.; Yin, G.-C. Degradation of rhodamine B by Fe(0)-based Fenton process with H_2O_2. *Chemosphere* **2011**, *83*, 1279–1283. [CrossRef]
43. Expósito, A.J.; Monteagudo, J.M.; Durán, A.; San Martín, I.; González, L. Study of the intensification of solar photo-Fenton degradation of carbamazepine with ferrioxalate complexes and ultrasound. *J. Hazard. Mater.* **2018**, *342*, 597–605. [CrossRef] [PubMed]
44. Kušić, H.; Lončarić Božić, A.; Koprivanac, N. Fenton type processes for minimization of organic content in coloured wastewaters: Part I: Processes optimization. *Dyes Pigm.* **2007**, *74*, 380–387. [CrossRef]
45. Pérez, M.; Torrades, F.; Domènech, X.; Peral, J. Fenton and photo-Fenton oxidation of textile effluents. *Water Res.* **2002**, *36*, 2703–2710. [CrossRef]
46. Ohno, M.; Ito, M.; Ohkura, R.; Mino A, E.R.; Kose, T.; Okuda, T.; Nakai, S.; Kawata, K.; Nishijima, W. Photochemical decomposition of perfluorooctanoic acid mediated by iron in strongly acidic conditions. *J. Hazard. Mater.* **2014**, *268*, 150–155. [CrossRef]
47. Desipio, M.M.; Van Bramer, S.E.; Thorpe, R.; Saha, D. Photocatalytic and photo-fenton activity of iron oxide-doped carbon nitride in 3D printed and LED driven photon concentrator. *J. Hazard. Mater.* **2019**, *376*, 178–187. [CrossRef]
48. Bavasso, I.; Montanaro, D.; Di Palma, L.; Petrucci, E. Electrochemically assisted decomposition of ozone for degradation and mineralization of Diuron. *Electrochim. Acta* **2020**, *331*, 135423. [CrossRef]